CRANE : Civil Engineering Research Journal
Volume 7 Nomor 2 Edisi Oktober 2026
E-ISSN: 2775-4588

IMPROVEMENT OF SOIL LIQUEFACTION BY MICRO-PILE AND SOIL GROUTING FOR LIQUEFACTION-INDUCED FLOWSLIDE: A NUMERICAL ASSESSMENT

Rina Rebut Rayhansah[1*], Muhsiung Chang[2] , Hsu-Jen Lin[2], Muhammad Hamzah Fansuri[3] , Togani Cahyadi Upomo[4] , Rini Kusumawardani[4]

[1]Department of Civil Engineering, Universitas Kadiri, Indonesia
[2]Department of Civil and Construction Engineering, National Yunlin University of Science and Technology, Taiwan
[3]Department of Civil Engineering, Universitas Pertahanan Republik Indonesia, Indonesia
[4]Department of Civil Engineering, Universitas Negeri Semarang, Indonesia
E-mail: rinarebutrayhansah@unik-kediri.ac.id*
*Corresponding author

ABSTRACT

Liquefaction-induced slope failure is a major geotechnical hazard caused by excess pore water pressure (EPWP) in spatially variable soils during earthquakes. However, comparative three-dimensional evaluations of mitigation methods remain limited. This study assesses the performance of micro-piles (MP) and soil grouting (GT) using three-dimensional finite element modeling in OpenSeesPL on a 30 m liquefiable slope subjected to CHY002 seismic input. Results indicate that the untreated slope (OG) developed EPWP of 72–75 kPa and lateral displacement of 26–27 m. MP reduced EPWP by 30–40% to 28–33 kPa and decreased displacement to 21–22 m. GT achieved greater EPWP reduction of 73–80% to 15–20 kPa, with comparable displacement reduction. The results show that treatment depth strongly governs mitigation effectiveness. GT is more effective in controlling pore pressure, whereas MP improves stiffness and redistributes seismic loads. These findings highlight the importance of depth-controlled design and provide a unified three-dimensional framework for evaluating liquefaction mitigation strategies in seismic slope engineering.

Keywords: Liquefaction, Ground improvement, Excess pore water pressure, Soil grouting, Seismic slope stability

ABSTRAK

Keruntuhan lereng akibat likuifaksi merupakan salah satu bahaya geoteknik utama yang disebabkan oleh terbentuknya tekanan air pori berlebih (excess pore water pressure/EPWP) pada tanah yang memiliki variasi spasial selama kejadian gempa. Namun, kajian komparatif tiga dimensi terhadap metode mitigasi likuefaksi masih relatif terbatas. Penelitian ini mengevaluasi kinerja mikro-tiang (micro-piles/MP) dan grouting tanah (soil grouting/GT) menggunakan pemodelan elemen hingga tiga dimensi dengan OpenSeesPL pada lereng likuifaksi setinggi 30 m yang dikenai input gempa CHY002. Hasil analisis menunjukkan bahwa lereng tanpa perkuatan (OG) menghasilkan EPWP sebesar 72–75 kPa dan perpindahan lateral sebesar 26–27 m. Penerapan mikro-tiang mampu menurunkan EPWP sebesar 30–40% menjadi 28–33 kPa serta mengurangi perpindahan lateral menjadi 21–22 m. Sementara itu, grouting tanah memberikan penurunan EPWP yang lebih besar, yaitu 73–80% menjadi 15–20 kPa, dengan pengurangan perpindahan lateral yang relatif sebanding. Hasil penelitian menunjukkan bahwa kedalaman perbaikan tanah sangat menentukan efektivitas mitigasi. Grouting tanah lebih efektif dalam mengendalikan tekanan air pori, sedangkan mikrotiang berperan dalam meningkatkan kekakuan dan mendistribusikan ulang beban seismik. Temuan ini menegaskan pentingnya desain berbasis kedalaman perbaikan serta menyediakan kerangka evaluasi tiga dimensi yang terpadu untuk menilai strategi mitigasi likuifaksi pada rekayasa lereng seismik.

Kata kunci: *Likuifaksi, Perbaikan tanah, Tekanan air pori berlebih, Grouting tanah, Stabilitas lereng seismik*

1. Introduction

Variability in soil properties plays a critical role in governing the mechanical response of geotechnical systems and introduces significant uncertainty in predicting ground behavior [1], [2], [3]. During seismic loading, spatially variable soils tend to generate higher excess pore water pressure

(EPWP), thereby accelerating strength degradation and increasing the likelihood of instability and ground failure toward weaker zones [4], [5], [6]. Earthquake-induced liquefaction has caused significant structural damage and casualties worldwide. This phenomenon occurs when saturated sandy soils subjected to cyclic or monotonic shear loading generate excess pore water pressure, leading to a substantial reduction in effective stress and shear strength, causing the soil to behave in a fluid-like manner, as described by Castro and Poulos. The increase in pore water pressure during strong ground shaking reduces effective stress within the soil skeleton, which may trigger ground deformation and instability. When liquefaction develops in sloping ground conditions, the soil mass may undergo lateral movement that results in flowslides or large ground displacement [11], failures commonly occur in loose, saturated, cohesionless soils during strong earthquakes. Historical events demonstrating these effects include the earthquakes in Chile (1960), Alaska (1964), Niigata in Japan (1964), Chi-Chi in Taiwan (1999), and Palu in Indonesia (2018) (Figure 1).

Among liquefaction mitigation approaches, this study focuses on micro-piles (MP) and soil grouting (GT), where several research gaps remain: (1) most studies emphasize fundamental liquefaction mechanisms rather than integrated mitigation performance [6], [10]; (2) analyses are predominantly conducted on level ground rather than sloping liquefiable conditions (M. Chang et al., 2021); (3) direct comparative studies between MP and GT within a unified framework are still limited [18], [19]; (4) key response parameters such as excess pore water pressure (EPWP) [2], lateral deformation, and settlement are rarely evaluated simultaneously [5]; (5) three-dimensional numerical simulations are still underutilized despite their importance in capturing complex soil behavior [4]; (6) experimental studies on slope failure due to liquefaction often lack integration with mitigation techniques [19] and (7) the applicability of existing findings to realistic and region-specific geotechnical conditions remains insufficient [1], [2], [20], [21], [22]. Ground improvement methods such as stone columns, high modulus columns, pile-pinning, and grouting have been proven effective in reducing liquefaction potential through the mitigation of excess pore pressure, settlement, and lateral displacement [8], [23], [24], [25]. However, most previous studies have been limited to level ground conditions and single foundation systems, with limited attention to liquefaction-induced flowslides on slopes, which involve loss of shear strength and downslope soil mass movement [2]. Research on pile-pinning generally focuses on pile bending, shear, and buckling behavior [26], whereas grouting studies mainly emphasize improvements in soil stiffness [27], [28], strength, and permeability [29], [30]. Three-dimensional numerical studies integrating micro-piles and soil grouting as a combined mitigation system remain scarce [26], particularly in evaluating the effects of design parameters on displacement, pore pressure ratio, and slope safety factor during earthquakes (Table 1).

Table 1. Relate works

Study	EPWP Control	Stiffness Increase	Deep Treatment Effect	Field Applicability	Outcome
[15], [19]	v				Sustainable concept, limited field validation
[2], [15]	v			v	EPWP governs liquefaction triggering mechanism
[5]	v		v	v	Deep systems effectively suppress deformation
[15]	v	v			Lateral resistance improved, liquefaction uncertain
Novelty (OG; MP; SG)	v	v	v	v	OG = Severe liquefaction (> 72kPa; 26–27 m) MP = EPWP > 29%, deformation > 20 m SG = EPWP >70%, deformation >20m

Source: [1], [2], [5], [15], [19]

This study focuses on liquefaction phenomena observed during the Chi-Chi earthquake in Taiwan. On September 21, 1999, a major earthquake with a moment magnitude of Mw = 7.6 struck central Taiwan, resulting in more than 2,300 fatalities and over 8,700 injuries. The event caused extensive

structural damage and widespread liquefaction throughout the affected region. Numerous liquefaction sites were documented by The National Center for Research on Earthquakes Engineering (NCREE) of Taiwan, particularly in the alluvial plains of Yuanlin, Nantou, and Wufeng [17]. Field investigations clearly reveal that liquefaction poses a critical threat to infrastructure, with more than 90% of over 1,000 documented cases involving building damage. Specifically, approximately 56% of the cases resulted in significant ground settlement, 31% led to structural tilting, and 13% caused complete building collapse [12]. These findings unequivocally demonstrate that liquefaction-induced ground failure is not only widespread but also severely destructive, particularly for structures founded on susceptible soil deposits.

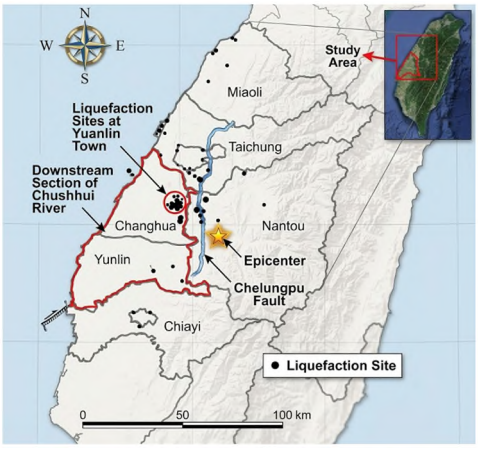

Figure 1. Liquefaction sites during the 1999 Chi-chi Earthquake, Taiwan [12]

To effectively mitigate liquefaction-induced damage, a wide range of ground improvement and soil reinforcement techniques have been rigorously developed and implemented. The most commonly adopted methods include stone columns (SC), geosynthetics-encased stone columns (ESC), MP, DS, solidification, GT, all of which aim to enhance soil strength, reduce excess pore water pressure, and improve overall ground stability under seismic loading [18]. These techniques aim to improve soil strength, stiffness, and drainage capacity in order to enhance the stability of liquefiable ground. Among these mitigation approaches, this study focuses on two techniques: MP and GT [10], [31], [32]. The selection of appropriate liquefaction mitigation methods largely depends on site conditions and soil characteristics. Although various ground improvement techniques have been developed to enhance soil strength and stability, most previous studies have primarily focused on individual methods or simplified soil conditions [33]. Comparative investigations evaluating the seismic performance of different mitigation techniques in liquefiable sloping ground remain limited. In particular, studies that simultaneously analyze the effectiveness of micro-piles and soil grouting using three-dimensional numerical simulations are still scarce. Therefore, a comprehensive evaluation of these mitigation techniques is necessary to better understand their influence on excess pore water pressure development and lateral deformation behavior during seismic loading. Therefore, this study systematically investigates the effectiveness of MP and GT in mitigating liquefaction-induced deformation through advanced three-dimensional numerical simulations. Key design parameters are rigorously evaluated, including pile diameter, spacing, and length for the micro-pile system, as well as improvement depth for the soil grouting technique. The analysis quantitatively examines their influence on EPWP evolution, lateral deformation mechanisms, and displacement profiles in mildly sloping liquefiable ground. This study contributes to the existing body of knowledge by providing a unified comparative framework for MP and GT, integrating multiple response parameters within a 3D modeling approach, and offering engineering insights into the selection of appropriate mitigation strategies under realistic geotechnical and seismic conditions

2. Methods

2.1. Research design

This study adopts a quantitative, simulation-based research design using three-dimensional finite element analysis to evaluate the seismic performance of liquefaction mitigation techniques [34]. The numerical modeling is conducted using OpenSeesPL, a well-established platform in earthquake geotechnical engineering that provides advanced constitutive models, boundary conditions, and dynamic analysis capabilities [26], [27], [28], [29], [30], [35], [36]. The model employs a 20–8 node element formulation, where 20 nodes represent the translational degrees of freedom of the soil skeleton and 8 corner nodes represent pore water pressure, enabling coupled solid–fluid interaction analysis. A representative soil column with a depth of 30 m is modeled, incorporating

periodic boundary conditions on vertical faces and fixed boundary conditions at the base. Seismic loading is applied at the base in the horizontal (X) direction [5]. The model configuration and boundary conditions are adopted based on previous validated studies using OpenSeesPL and FEM-based liquefaction analysis to ensure numerical robustness [13], [34].

2.2. Population and sampling

The study uses a representative soil profile from the Chuoshui River alluvial fan delta in Taiwan, specifically Borehole W5-3, which has been widely reported as liquefaction-prone during the Chi-Chi Earthquake 1999 [12]. The soil profile consists of layered deposits including very loose sand, loose sand, medium sand, clay, and silt, with groundwater level at 3.84 m depth.

Sampling in this study is defined as the selection of critical soil layers and observation points within the numerical domain, including center and boundary locations of the soil column, as well as a depth of 7 m to capture liquefaction response [2], [4], [36]. The seismic input motion is derived from the CHY002 station record (Mw 7.6) and processed deconvolution to obtain input motion at 30 m depth, ensuring consistency with subsurface boundary conditions.

2.3. Instrument and Prosedure

The primary research instrument is OpenSeesPL, which is used to perform 3D dynamic finite element simulations. The model incorporates: (a) Nonlinear soil constitutive behavior; (b) EPWP; (c) Multi-layer soil stratigraphy (11 layers up to 30 m depth); (d) Two mitigation systems: MP and GT [12], [37] (Fig. 2, 3, 4).

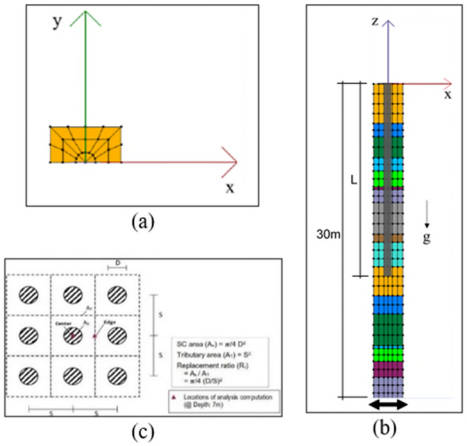

Figure 2. Representative FE meshes of the soil column for MP numerical simulation

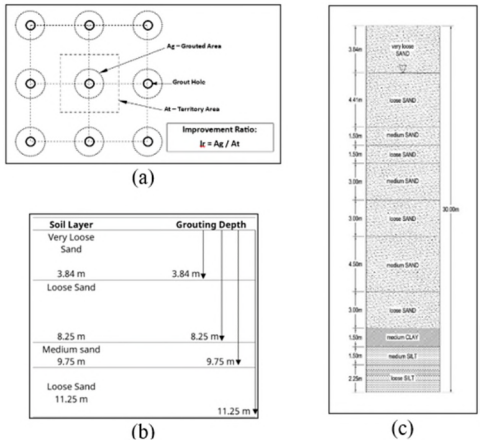

Figure 3. Improvement ratio and depth of soil deposit for GT numerical simulation

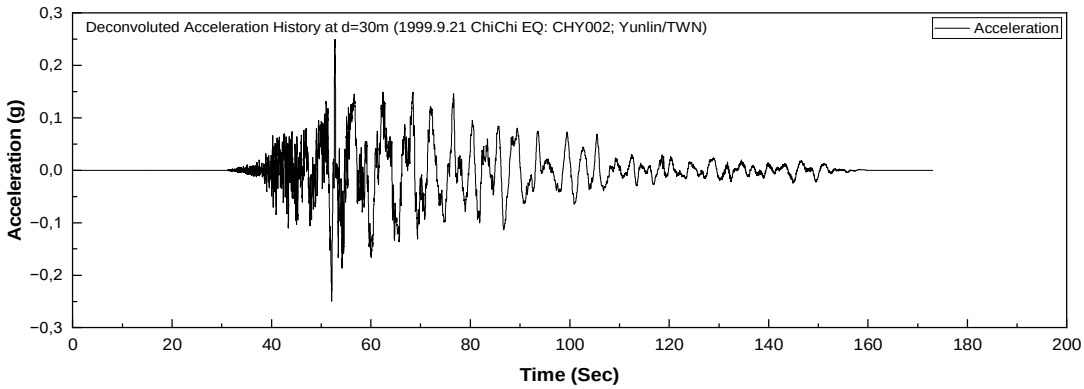

Figure 4. Deconvoluted acceleration time history at 30 m deep adopted as the input motion for OpenSeesPL analysis (1999.9.21 ChiChi EQ; CHY002; EW, PGA=0.249g).

To evaluate the seismic response of liquefiable soils, a representative profile from the Chuoshui River alluvial fan–delta in Taiwan was selected and analyzed using the CRAFD method [12]. At Borehole W5-3, the groundwater table is located at 3.84 m depth, with stratigraphy consisting of loose to medium sand overlying clay and silt layers, making it highly susceptible to liquefaction under seismic loading. Soil properties derived from subsurface investigations (SPT/ CPT) are used to determine the cyclic resistance ratio (CRR), which is incorporated into a three-dimensional finite element model in OpenSeesPL [38], [39], [40]. The model consists of 11 soil layers up to 30 m depth, with seismic motion applied at the base. Two mitigation techniques are evaluated: MP and GT, each defined by specific design parameters. Micro-piles function as reinforcement elements that improve slope stability and reduce lateral deformation, although they may not fully suppress excess pore water pressure (EPWP), with their performance strongly dependent on site conditions [37]. In contrast, soil grouting enhances soil strength and reduces permeability by injecting materials such as cement–bentonite, making it effective for weak or heterogeneous deposits [2]. The grouted soil properties are estimated using a composite formulation based on the improvement ratio, integrating original and treated soil characteristics. For soil grouting, composite material properties are estimated using the mixture formulation [7], [18], [19].

$$P = (1\text{-}Ir)\ Ps + (Ir)\ Pg \quad (1)$$

The improvement ratio, Ir, represents the ratio of the grouted area (Ag) to the territory area (At) of the grouted hole, as shown in picture 3. The soil properties considered in this estimation include parameters such as: γ_m, Gmax, Bmax, B, ϕ, ϕ_T, c, K, and other liquefaction-related parameters (c1, d1, d2, l1, l2, l3).

The physical properties of the original soil deposit are detailed (Table 2), whereas those of the grouted soil deposit are shown (Table 3). The estimated composite properties for an improvement ratio of 40% with grouting depths (d1 (3.84 m); d2 (8.25 m); d3 (11.25)) are illustrated (Table 3). This table highlights the composite material properties (P) for the grouted soil option. An analysis of the liquefaction potential area using numerical results confirms that the installation of soil grouting can effectively prevent lateral displacement. As mentioned in the previous paragraph, the effectiveness of this mitigation strategy is highly dependent on the specific site conditions, including the type of soil and groundwater level.

To improve methodological transparency, the OpenSeesPL model was validated using previously established liquefaction studies and by comparing the untreated ground (OG) response with documented behavior of the 1999 Chi-Chi Earthquake, including high excess pore water pressure (EPWP), lateral spreading, and large deformation in loose saturated alluvial soils. Material parameters such as shear modulus (Gmax), bulk modulus (Bmax), hydraulic conductivity (Ksoil), friction angle (ϕ), cohesion (c), and liquefaction constants (c1, d1, d2, l1, l2, l3) were calibrated from available SPT/CPT data, empirical correlations, and published parameter ranges. For grouted zones, equivalent composite properties were estimated using the improvement-ratio approach between treated and untreated soil. The finite element mesh was refined near surface layers and improvement zones to capture stress concentration and pore pressure changes, while periodic boundaries on vertical sides minimized wave reflection and a fixed base received the horizontal seismic input motion. The analysis assumes laterally continuous soil layers, constant groundwater level, homogeneous grouted material, and one-directional earthquake loading, which are considered appropriate for comparative evaluation of liquefaction mitigation performance (Figure 5).

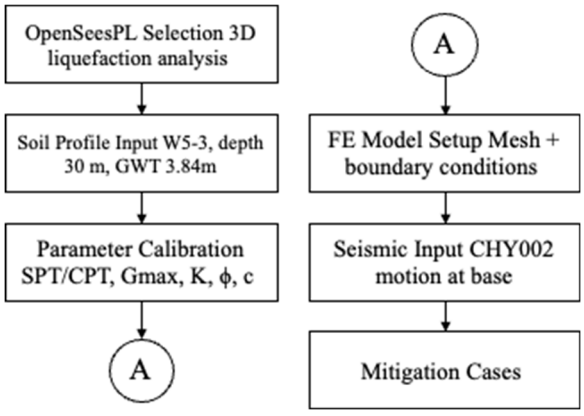

Figure 5. Flowchart

CRANE : Civil Engineering Research Journal
Volume 7 Nomor 2 Edisi Oktober 2026
E-ISSN: 2775-4588

Table 2. Material parameter of the original soil deposit (Original ground; OG) and liquefaction mitigation options

Parameters	Unit	Very Loose	Loose	Medium	Loose	Medium	Medium Clay	
		SAND			SILT			Micro-Pile
		Original Soil Deposit						
γ	KN/m^3	15.94	19.26	19.23	17.76	19.91	18.54	24.5
ϕ	deg	29	29	33	29	0	33	-
c	KPa	-	-	-	-	-	37	-
ϕ_{PT}	deg	29	29	27	29	29	27	-
G_{max}	KPa	5.50E+04	5.50E+04	7.50E+04	5.50E+04	7.50E+04	5.50E+04	1.40E+07
B_{max}	KPa	1.50E+05	1.50E+05	2.00E+05	1.50E+05	2.00E+05	3.00E+05	
K_{soil}	m/s	6.60E-05	6.60E-05	6.60E-05	6.60E-07	6.60E-07	6.60E-09	
E_r	KPa	-	-	-				3.50E+07
ν		-	-	-				0.2
σ_{py}		-	-	-				5.20E+04

*Note: γ = unit weight; ϕ = friction angle; c = cohesion; ϕ_{PT} = phase transformation friction angle; Gmax = shear modulus at a references effective confining pressure of 80 kPa; Bmax – bulk modulus at a references effective confining pressure of 80 kPa; Ksoil = hydraulic conductivity of soil; Er = young's modulus at a references effective confining pressure of 80 kPa; ν = Poisson's ratio; σ_{py} = yield stress.
Source: data processing (2026)

Table 3. Material Properties (PG and P)

Parameter	Unit	Material properties of grouted soils (PG)				Material properties of composite soils (P)			
		SAND							
		Very Loose	Loose	Medium	Loose	Very Loose	Loose	Medium	Loose
Thickness	m	3.84*	8.25*	9.75*	11.25*	3.84	8.25	9.75	11.25
$\boldsymbol{\gamma_m}$	kN/m^3	16.76*	19.56*	19.54*	19.48*	18	20	20	20
G_{max}	(kPa)	63.8E2*	63.8E2*	87.E3*	63.8E2*	7.70E+04	7.70E+04	1.05E+05	7.70E+04
B_{max}	(kPa)	174.E3*	174.E3*	232.E3*	174.E3*	2.10E+05	2.10E+05	2.80E+05	2.10E+04
B	(kPa)	2.55E3*	2.55E3*	2.55E3*	2.55E3*	3.08E+03	3.08E+03	3.08E+03	3.08E+03
$\boldsymbol{\phi}$	Deg	29*	29*	33*	29*	29	29	33	29
$\boldsymbol{c\sqrt{3/2}}$	(kPa)	68.12*	68.18*	68.18*	68.18*	170	170	170	170
K	m/s	5.2E-5*	5.2E-5*	5.2E-5*	5.2E-5*	3.0E-5	3.0E-5	3.0E-5	3.0E-5
$\boldsymbol{\phi_{PT}}$	deg	29*	29*	27*	29*	29	29	27	29
c1	(kPa)	0.21	0.21	0.07	0.21	0.21	0.21	0.07	0.21
d1	(kPa)	0	0	0.4	0	0	0	0.4	0
d2	(kPa)	0	0	2	0	0	0	2	0
l1	(kPa)	10	10	10	10	10	10	10	10
l2	(kPa)	0.02	0.02	0.02	0.02	0.02	0.02	0.02	0.02
l3	(kPa)	1	1	1	1	1	1	1	1

*Note: MOI, Taiwan (2017). Design Code for Foundation Structures. For grouted sandy soil with low-strength hardener: "γ_t"20kN/m^3; "c"200kPa; "ϕ"no change; "E_{50}"100MPA; Emax2E_{50}; "ν"0.3 G = E / [2(1+2v)]; B = E / [3(1-2v)]

3. Results and Discussion

The subsequent section presents an analysis of the numerical simulation results to evaluate the effectiveness of the proposed liquefaction mitigation techniques. The discussion focuses on the development of excess pore water pressure (EPWP), lateral deformation time histories, and displacement profiles within the soil deposits.

3.1. Results

The untreated ground showed severe liquefaction potential, with EPWP rapidly rising to 72–75 kPa, indicating major effective stress loss. Longer micro-piles reduced peak EPWP to 52–72 kPa and improved dissipation by increasing stiffness and transferring stress to deeper stable

CRANE : Civil Engineering Research Journal
Volume 7 Nomor 2 Edisi Oktober 2026
E-ISSN: 2775-4588

layers. Deep soil grouting was the most effective method, lowering EPWP to 15–20 kPa, equivalent to a 73–80% reduction compared with untreated ground.

The computed response shows that the OG produced the minimum cumulative lateral displacement demand, reaching approximately 5 m at 170 s, whereas both ground-improvement systems resulted in substantially higher displacement demands throughout the seismic excitation period (Figure 7). Lateral displacement increased after 55 s in all cases, but untreated ground showed the largest movement of 26–27 m within the upper 0–6 m liquefiable layer. Longer micro-piles and deeper grouting reduced final displacement to about 21 m by improving stiffness and anchorage in stable layers. This indicates that deeper treatment is more effective for controlling sliding and post-liquefaction ground movement (Figure 8). Both mitigation methods reduced upper-zone displacement, but the deepest treatments gave the best performance at about 21–22 m. Long micro-piles worked by transferring lateral loads to deeper competent layers, while deep grouting reduced movement through densification and bonding. The displacement inflection at 22–24 m depth marks the boundary between the moving liquefied layer and the stable base soil.

Numerical responses indicate that system behavior is primarily governed by EPWP evolution and lateral deformation, both of which are strongly dependent on improvement depth. Initially, EPWP increases rapidly from 40–45 s to a peak of 72–75 kPa at 55–65 s, representing the critical point of effective stress loss. In the micro-pile system, high

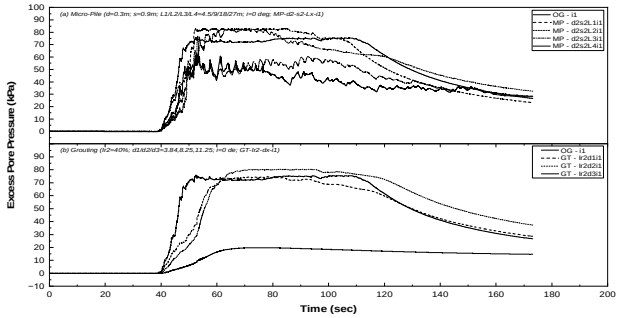

Figure 6. EPWP time histories at 7 m depth for OG, MP, and GT under seismic loading.

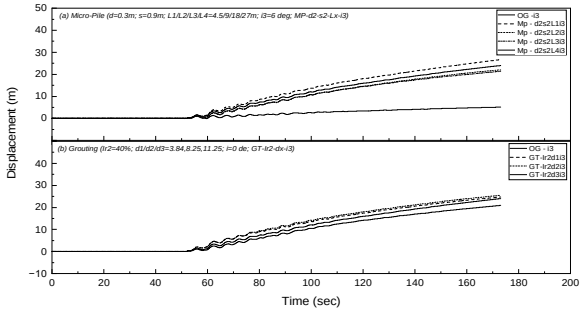

Figure 7. Lateral displacement time histories at 7 m depth for OG, MP, and GT on sloping ground during seismic loading.

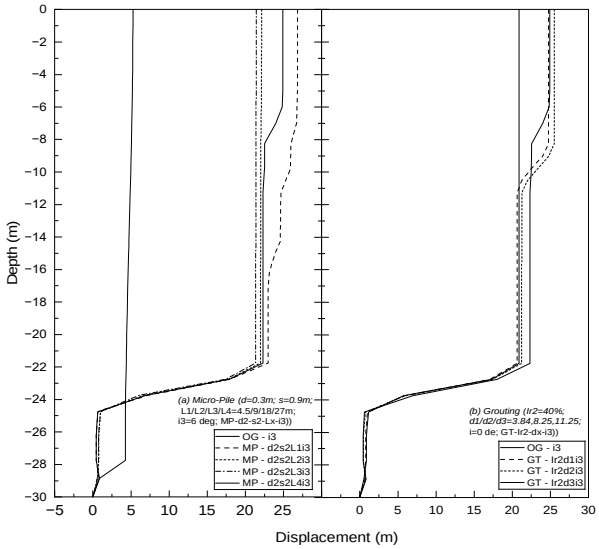

Figure 8. Final lateral displacement profiles with depth for OG, MP, and GT after seismic loading.

3.2. Discussion

EPWP is still observed for short piles (75–83 kPa for 4.5–9 m), while longer piles (18–27 m) reduce the peak to 52–72 kPa, with residual pressure decreasing to 28–33 kPa at 170 s, corresponding to an approximate 40% reduction from the initial peak condition (Table 4).

Table 4. EPWP Response and Lateral Deformation under Different Ground Improvement Systems

System	Depth / Parameter	Peak EPWP (kPa)	Residual EPWP (170 s)	Maximum Lateral Deformation (m)	EPWP Reduction	Deformation Reduction
OG		72–75		26–27		
Micro-pile (MP)	4.5–9 m	75–83		25–26	0%	5–8%
	18–27 m	52–72	28–33	21–22	30–40%	15–19%
Soil grouting (SG)	3.84 m	72–75		25–26	0–5%	5–8%
	8.25 m	30–35		22–24	50–60%	10–15%
	11.25 m	15–20		21–22	73–80%	15–19%

This study confirms previous liquefaction research that ground failure is driven by EPWP buildup and effective stress loss, requiring efficient and practical mitigation strategies [1], [2]. Literature highlights efficient, practical, sustainable seismic stabilization [5], [15], [19]. Numerical results show micro-piles and grouting reduce EPWP 80% and displacement 26–27 m to 21–22 m effectively (Table 5).

Table 5. Integrated Literature and Present Study on Liquefaction Mitigation and Foundation Response

Study	System	Mechanism	Finding	Implication
[1], [2], [15], [19]	Mitigation	Bonding and desaturation	Improves liquefaction resistance but limited by efficiency and field applicability	Promising sustainable method, needs further validation
[1], [2], [15]	General mitigation	EPWP reduction and effective stress recovery	Liquefaction governed by EPWP increase; need practical, low-impact solutions	Emphasis on cost-effective mitigation
[5]	drains, walls, deep mixing	Stiffness increase and confinement	Deep systems outperform shallow treatment in reducing deformation	Full-depth improvement is critical
Present study	OG condition	EPWP generation and instability	EPWP 72–75 kPa, deformation 26–27 m	Confirms high liquefaction vulnerability
	Micro-pile (MP)	Stiffness and stress redistribution	EPWP reduced 30–40%, deformation 21–22 m (deep MP)	Moderate, depth-dependent performance
	Soil grouting (SG)	Densification & pore pressure suppression	EPWP reduced up to 73–80%, deformation 21–22 m	Most effective in EPWP control
	Integration	Depth-controlled mitigation	Deep treatment governs performance across studies	Confirms depth as key design parameter

Source: data processing (2026)

Deep treatment depth is the key factor controlling liquefaction mitigation performance. Soil grouting at 11.25 m was most effective in reducing EPWP by up to 73–80%, while both deep grouting and long micro-piles achieved similar lateral deformation control, reducing displacement from 26–27 m to about 21–22 m (15–19%). This indicates that grouting is superior for pore pressure suppression, whereas both methods are effective for deformation control when treatment penetrates the liquefiable layer.

4. Conclusion

The untreated slope experienced severe liquefaction, shown by high EPWP (72–75 kPa) and extreme lateral displacement (26–27 m), indicating flowslide failure under seismic loading. Both mitigation methods improved stability, but through different mechanisms. Micro-piles mainly reduced deformation by increasing stiffness and transferring loads to deeper stable layers, while soil grouting was more effective in suppressing pore pressure, reducing EPWP by up to 73–80%. Although both methods lowered displacement to about 21–22 m, treatment depth proved to be the key controlling factor. Therefore, mitigation design should prioritize full coverage of the liquefiable layer and select methods based on performance objectives: micro-piles for deformation control, soil grouting for liquefaction resistance.

References

[1] P. E. Mergos and A. G. Sextos, "Selection of earthquake ground motions for multiple objectives using genetic algorithms," *Eng. Struct.*, vol. 187, no. July 2018, pp. 414–427, 2019, doi: 10.1016/j.engstruct.2019.02.067.

[2] A. G. Papadimitriou, A. I. Valsamis, and T. G. Limnaiou, "Liquefaction mitigation methods for existing shallow-founded elongated structures on horizontal or mildly-inclined ground," *Soil Dyn. Earthq. Eng.*, vol. 162, no. August, p. 107453, 2022, doi: 10.1016/j.soildyn.2022.107453.

[3] C. Y. Liu, C. Y. Ku, T. Y. Wu, Y. J. Chiu, and C. W. Chang, "Liquefaction susceptibility mapping using artificial neural network for offshore wind farms in Taiwan," *Eng. Geol.*, vol. 351, no. February, p. 108013, 2025, doi: 10.1016/j.enggeo.2025.108013.

[4] R. Popescu and P. Chakrabortty, "Mechanism of seismic liquefaction for heterogeneous soil," *Soil Dyn. Earthq. Eng.*, vol. 176, no. November 2023, p. 108339, 2024, doi: 10.1016/j.soildyn.2023.108339.

[5] J. S. Rajeswari and R. Sarkar, "Adequacy of batter piles under seismic conditions: A review of past performances and investigations," *Structures*, vol. 61, no. February, p. 106022, 2024, doi: 10.1016/j.istruc.2024.106022.

[6] L. Lu, Y. Xu, J. Tang, and G. Hu, "High-resolution satellite imagery analysis of coseismic landslides and liquefaction induced by the 2024 MW 7.4 Hualien earthquake, Taiwan, China," *Earthq. Res. Adv.*, vol. 5, no. 3, p. 100356, 2025, doi: 10.1016/j.eqrea.2024.100356.

[7] R. Popescu and P. Chakrabortty, "Mechanism of seismic liquefaction for heterogeneous soil," *Soil Dyn. Earthq. Eng.*, vol. 176, no. July 2023, p. 108339, 2024, doi: 10.1016/j.soildyn.2023.108339.

[8] D. Liu, L. Huang, J. Li, and Q. Shen, "Formulation and performance of nano-composite clay-cement based grouting materials in water-bearing sandy soil," *Case Stud. Constr. Mater.*, vol. 21, no. August, p. e03891, 2024, doi: 10.1016/j.cscm.2024.e03891.

[9] Y. F. Lee, Y. Y. Chi, C. H. Juang, and D. H. Lee, "Annual probability and return period of soil liquefaction in Yuanlin, Taiwan attributed to Chelungpu Fault and Changhua Fault," *Eng. Geol.*, vol. 114, no. 3–4, pp. 343–353, 2010, doi: 10.1016/j.enggeo.2010.05.012.

[10] W. J. Chang, S. H. Ni, A. Bin Huang, Y. H. Huang, and Y. Z. Yang, "Geotechnical reconnaissance and liquefaction analyses of a liquefaction site with silty fine sand in Southern Taiwan," *Eng. Geol.*, vol. 123, no. 3, pp. 235–245, 2011, doi: 10.1016/j.enggeo.2011.09.003.

[11] X. Feng, B. Ye, J. He, H. Miao, and C. Lin, "Shaking table test on underwater slope failure induced by liquefaction," *Soils Found.*, vol. 63, no. 4, p. 101357, 2023, doi: 10.1016/j.sandf.2023.101357.

[12] M. Chang, C. ping Kuo, R. eeh Hsu, S. hui Shau, and T. mei Lin, "Liquefaction potential and post-liquefaction settlement evaluations of the Chuoshui River Alluvial Fan in Taiwan," *Bull. Eng. Geol. Environ.*, vol. 71, no. 2, pp. 325–336, 2012, doi: 10.1007/s10064-011-0390-7.

[13] W. S. Chen *et al.*, "1999 Chi-Chi earthquake: A case study on the role of thrust-ramp structures for generating earthquakes," *Bull. Seismol. Soc. Am.*, vol. 91, no. 5, pp. 986–994, 2001, doi:

10.1785/0120000731.

[14] C. Hsein Juang, S. Hui Yang, H. Yuan, and S. Y. Fang, “Liquefaction in the Chi-Chi Earthquake-Effect of Fines and Capping Non-Liquefiable Layers,” *Soils Found.*, vol. 45, no. 6, pp. 89–101, 2005.

[15] K. Wang, S. Wu, and J. Chu, “Mitigation of soil liquefaction using microbial technology: An overview,” *Biogeotechnics*, vol. 1, no. 1, p. 100005, 2023, doi: 10.1016/j.bgtech.2023.100005.

[16] A. H. Vakili, A. Khajeh, M. M. Shalchian, and R. Tajari, “Experimental analysis of parameters affecting the lateral resistance of micropile groups embedded in sandy soil,” *Results Eng.*, vol. 27, no. March, p. 105663, 2025, doi: 10.1016/j.rineng.2025.105663.

[17] M. Chang, C. Kuo, R. Hsu, S. Shau, and T. Wu, “Assessment on Liquefaction Potential of the Mid-West Alluvial Plain During the 1999 Chi-Chi Earthquake , Taiwan Estimación del Potencial de Licuación de la Llanura Aluvial del Medio Oeste Durante el Terremoto de Chi-Chi , Taiwán en 1999,” no. May, 2021.

[18] M. H. Fansuri, M. Chang, H. Lin, R. R. Rayhansyah, T. C. Upomo, and R. Kusumawardani, “A Comparative Study of Seismic Performance Evaluation of Stone Column , Micro-Pile , and Geosynthetic-Encased Stone Column for Liquefaction Flowslide Mitigation,” 2022.

[19] X. Bao, Z. Jin, H. Cui, X. Chen, and X. Xie, “Soil liquefaction mitigation in geotechnical engineering: An overview of recently developed methods,” *Soil Dyn. Earthq. Eng.*, vol. 120, no. January, pp. 273–291, 2019, doi: 10.1016/j.soildyn.2019.01.020.

[20] T. A. Pham, S. Nadimi, and M. Sutman, “Softening-based interface model and nonlinear load-settlement response analysis of piles in saturated and unsaturated multi-layered soils,” *Comput. Geotech.*, vol. 171, no. April, p. 106331, 2024, doi: 10.1016/j.compgeo.2024.106331.

[21] S. L. Kramer, S. S. Sideras, and M. W. Greenfield, “The timing of liquefaction and its utility in liquefaction hazard evaluation,” *Soil Dyn. Earthq. Eng.*, vol. 91, pp. 133–146, 2016, doi: 10.1016/j.soildyn.2016.07.025.

[22] H. Zi, Z. Ding, X. Ji, Z. Liu, and C. Shi, “Effect of voids on the seismic vulnerability of mountain tunnels,” *Soil Dyn. Earthq. Eng.*, vol. 148, no. June, p. 106833, 2021, doi: 10.1016/j.soildyn.2021.106833.

[23] C. Wang, S. Han, J. Wu, Y. Wang, and J. Liao, “Study on the degradation mechanism of polyacrylate-composite grouting materials under sulfate attack,” *Constr. Build. Mater.*, vol. 505, no. December, pp. 1–11, 2025, doi: 10.1016/j.conbuildmat.2025.144705.

[24] Y. Tan *et al.*, “Research on microstructure and physico-mechanical properties of grouting materials based on nano calcium carbonate-polyurethane composite modification,” *Results Eng.*, vol. 28, no. October, p. 107974, 2025, doi: 10.1016/j.rineng.2025.107974.

[25] L. Bian, Q. Zhou, L. Ding, J. Zhang, and F. Chen, “Preparation and reinforcement performance of composite sodium silicate-based grouting materials for glacial till,” *Results Eng.*, vol. 29, no. July 2025, p. 109012, 2026, doi: 10.1016/j.rineng.2026.109012.

[26] M. H. Fansuri *et al.*, “Effects of various factors on behaviors of piles and foundation soils due to seismic shaking,” *Solid Earth Sci.*, vol. 7, no. 4, pp. 252–267, 2022, doi: 10.1016/j.sesci.2022.09.001.

[27] D. Forcellini, “Soil-structure interaction analyses of shallow-founded structures on a potential-liquefiable soil deposit,” *Soil Dyn. Earthq. Eng.*, vol. 133, no. March, p. 106108, 2020, doi: 10.1016/j.soildyn.2020.106108.

[28] L. Li, D. Huang, F. Jin, and S. Du, “Evaluation of synthetic and recorded ground motions for soil liquefaction analyses,” *Soil Dyn. Earthq. Eng.*, vol. 149, no. May, p. 106815, 2021, doi: 10.1016/j.soildyn.2021.106815.

[29] A. Asgari, M. Oliaei, and M. Bagheri, “Numerical simulation of improvement of a liquefiable soil layer using stone column and pile-pinning techniques,” *Soil Dyn. Earthq. Eng.*, vol. 51, pp. 77–96, 2013, doi: 10.1016/j.soildyn.2013.04.006.

[30] T. Mo, Q. Wu, D. Q. Li, and W. Du, “Influence of ground motion characteristics (velocity pulse and duration) on the pile responses in liquefiable soil deposits,” *Soil Dyn. Earthq. Eng.*, vol. 159, no. November

2021, p. 107330, 2022, doi: 10.1016/j.soildyn.2022.107330.

[31] S. Pal and K. Deb, "Effect of clogging of stone column on drainage capacity during soil liquefaction," *Soils Found.*, vol. 59, no. 1, pp. 196–207, 2019, doi: 10.1016/j.sandf.2018.10.005.

[32] E. M. El Sherbiny and J. T. Wang, "Stone column strategies for mitigating liquefaction-induced uplift of tunnels," *Soil Dyn. Earthq. Eng.*, vol. 187, no. September, 2024, doi: 10.1016/j.soildyn.2024.108961.

[33] Y. Sun, C. Li, and D. Jin, "A novel nonlinear model for liquefaction potential assessment of stone column-improved ground incorporating multiple factors," *Soil Dyn. Earthq. Eng.*, vol. 201, no. November 2025, p. 109966, 2026, doi: 10.1016/j.soildyn.2025.109966.

[34] M. M. Rahman, T. T. Nahar, and D. Kim, "FeView: Finite element model (FEM) visualization and post-processing tool for OpenSees," *SoftwareX*, vol. 15, p. 100751, 2021, doi: 10.1016/j.softx.2021.100751.

[35] M. Chang, H. J. Lin, R. R. Rayhansah, M. H. Fansuri, T. C. Upomo, and R. Kusumawardani, "Assessment on the improvement of liquefiable ground by stone-column, micro-pile and densification measures," *Smart Geotech. Smart Soc.*, pp. 563–566, 2023, doi: 10.1201/9781003299127-70.

[36] S. Demir and P. T. Özener, "Parametric investigation of effectiveness of high modulus columns in liquefaction mitigation," *Soil Dyn. Earthq. Eng.*, vol. 139, no. June, 2020, doi: 10.1016/j.soildyn.2020.106337.

[37] M. C. Capatti, D. Roia, S. Carbonari, and F. Dezi, "Micropile foundation subjected to dynamic lateral loading," *Procedia Eng.*, vol. 199, pp. 2324–2329, 2017, doi: 10.1016/j.proeng.2017.09.208.

[38] M. Chang, C. ping Kuo, S. hui Shau, and R. eeh Hsu, "Comparison of SPT-N-based analysis methods in evaluation of liquefaction potential during the 1999 Chi-chi earthquake in Taiwan," *Comput. Geotech.*, vol. 38, no. 3, pp. 393–406, 2011, doi: 10.1016/j.compgeo.2011.01.003.

[39] J. H. Hwang, S. Khoshnevisan, C. H. Juang, and C. C. Lu, "Soil liquefaction potential evaluation – An update of the HBF method focusing on research and practice in Taiwan," *Eng. Geol.*, vol. 280, no. August 2020, p. 105926, 2021, doi: 10.1016/j.enggeo.2020.105926.

[40] K. Nakai, I. Khan, and T. Noda, "Experiments and elastoplastic analyses on soil disturbance of soft clay subjected to cyclic loading," *Can. Geotech. J.*, pp. 1–15, 2026, doi: 10.1139/cgj-2025-0284.

[41] [42] D. Christodoulou, P. Lokkas, I. Markou, A. Droudakis, I. Chouliaras, and N. Alamanis, "Principles and Developments in Soil Grouting: a Historical Review," *WSEAS Trans. Adv. Eng. Educ.*, vol. 18, no. December, pp. 175–191, 2021, doi: 10.37394/232010.2021.18.18.